Bioorganic & Medicinal Chemistry Letters 21 (2011) 3479–3482

Contents lists available at ScienceDirect

Bioorganic & Medicinal Chemistry Letters

journal homepage: www.elsevier.com/locate/bmcl

Design, synthesis, and biological activity of novel Magmas inhibitors

Paul T. Jubinsky [a,b,*], Mary K. Short [b], Mohmoud Ghanem [c], Bhaskar C. Das [b,d,*]

[a] Pediatric Hematology/Oncology, Yale University Medical School, New Haven, CT 06510, United States
[b] Department of Developmental & Molecular Biology, Albert Einstein College of Medicine, Bronx, NY 10461, United States
[c] Department of Biochemistry, Albert Einstein College of Medicine, Bronx, NY 10461, United States
[d] Department of Nuclear Medicine, Albert Einstein College of Medicine, Bronx, NY 10461, United States

ARTICLE INFO

Article history:
Received 29 January 2011
Revised 10 March 2011
Accepted 14 March 2011
Available online 21 March 2011

Keywords:
Magmas inhibitors
Guanidine pharmacophores
Chemical genetics
LRD-limited
Rational design
Molecular modeling
Tim16
Pam16
Mitochondrial protein import

ABSTRACT

Magmas (mitochondria associated, granulocyte–macrophage colony stimulating factor signaling molecule), is a highly conserved and essential gene, expressed in all cell types. We designed and synthesized several small molecule Magmas inhibitors (SMMI) and assayed their effects on proliferation in yeast. We found that the most active compound **9** inhibited growth at the 4 μM scale. This compound was shown by fluorometric titration to bind to Magmas with a K_d = 33 μM. Target specificity of the lead compound was established by demonstrating direct binding of the compound to Magmas and by genetic studies. Molecular modeling suggested that the inhibitor bound at the predicted site in Magmas.

Our laboratory identified Magmas (mitochondria associated granulocyte–macrophage colony stimulating factor signaling molecule), as a GM-CSF inducible gene in myeloid cells.[1] Magmas protein localizes to the inner membrane of mitochondria, and protein expression is both developmentally regulated and tissue specific.[2] The protein is highly conserved, and is required for mitochondria function and cell survival.[3] Immuno-precipitation and immuno-affinity chromatography studies show that Magmas mostly associates with other mitochondrial proteins. Reduction in Magmas expression results in decreased mitochondrial function (Soumit Roy and Jubinsky, unpublished data).

The yeast ortholog of Magmas, known as Tim16 or Pam16 has been shown to functionally interact with another protein, Tim14, to regulate the importation of peptides into the mitochondria through an import complex.[4] Studies have established that the functional Tim14/Tim16 complex is a heterodimer.[4b,5]

Magmas expression in prostate cancer samples suggested a role for this protein in human cancer.[6] Magmas staining is minimal to absent in normal prostate tissue by immuno-histochemistry. Elevated levels of Magmas protein occurred in a subset of advanced-grade, invasive adenocarcinoma. However, many samples of similar stage and grade had staining patterns identical to normal prostate epithelium. Increased staining resulted from higher amounts of Magmas in the abnormal cells and not from increased numbers of mitochondria. It indicates that the Magmas expression may affect response to therapy, possibly by altering mitochondrial function. Data from other laboratories also supports the importance of Magmas expression in human cancer.[7]

Based on the above findings, we believed that small molecule Magmas inhibitors (SMMI) could be beneficial for studying mitochondrial function and for diagnosing and treating human disease. The design of potential compounds was aided by analyzing information known about the structure of Magmas derived from crystallography data.[5a]

Small molecules likely to interact with highly conserved functional regions of Magmas were conceived and a corresponding small chemical library containing oxazine, chromene and guanidine pharamacophore groups were synthesized. Instead of the large libraries typically used in high-throughput screening our library consists of 10 lead compounds likely to contain a fairly complete range of structural motifs that interact with Magmas. We have termed this method the 'limited design approach'

The biological activity of the compounds was tested in *Saccharomyces cerevisiae* proliferation assays. Human Magmas

* Corresponding authors. Tel.: +203 785 2754; fax: +203 737 2228 (P.T.J.); tel.: +1 17184302422; fax: +1 17184308853 (B.C.D.)
E-mail addresses: paul.jubinsky@yale.edu (P.T. Jubinsky), bdas@aecom.yu.edu (B.C. Das).

0960-894X/$ - see front matter © 2011 Elsevier Ltd. All rights reserved.
doi:10.1016/j.bmcl.2011.03.050

and Tim16 share 42% amino acid identity, and human Magmas is able to functionally replace endogenous Tim16.[8]

Our small molecule library (Scheme 1) was synthesized by the chemical modification of existing reactions.[9] The chemical synthesis of lead compound **9** is shown in (Scheme 2).

In brief, acid **16** was reacted with guanidine hydrochloride,1,1′carbonyldiimidazole in DMF–dioxane mixture. The crude reaction mixture was evaporated and the residue was purified by fractional crystallization from methanol, to give compound **9** white crystals mp 165–167 °C.[10]

A library of randomized mutations in yeast Magmas (*TIM16*) were made by error-prone PCR. The genes encoding the mutations were spliced into plasmid pRS315 and introduced into a haploid yeast strain containing a wild-type copy of *TIM16* on plasmid pRS316 and a null genomic replaced by a *HIS3* cassette. The plasmid containing the wild type (wt) *TIM16* gene was lost by selection in media containing FOA[11] and two mutants were identified for having altered sensitivity to SMMI (small molecule Magmas inhibitor) **9** in proliferation assays. The mutations in *TIM16* were determined from DNA sequencing of the plasmid from each mutant strain and were found to result in amino acid changes N84T and A104S in Tim16.

S. cerevisiae strain J47D in log phase growth was plated in 96 well dishes at 1.5×10^4 cells/well in YEPD media. Magmas inhibitors were diluted in DMSO and added at various concentrations (range 0–1 mM) to each well in triplicate at a final DMSO concentration of 1%. Samples were cultured at 30 °C in a Bioscreen C MBR incubator (Growth Curves USA, Piscataway, NJ) and optical density (OD) readings at 600 nM were measured every 30 min for the indicated time in the plots. Cell proliferation data was analyzed and plotted using Microsoft Excel. Standard deviations were smaller than 2% of the mean OD value ($n = 3$) and each experiment was performed at least two independent times.

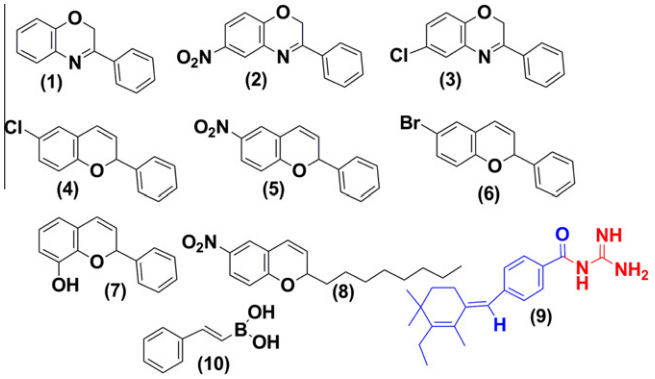

Scheme 1. Small focused molecular library (1–10).

The fluorescence emission spectra ($\lambda_{exc} = 295$ nm, 2.5 nm slit width, and 10 mm path length) of free or ligand bound Magmas (yeast or mouse) were acquired using a FluroMax-3 spectrofluorometer thermostated at 25 °C. The dissociation constants for compound **9** were obtained from the fluorometric titrations of the yeast or mouse Magmas (3 μM) with compound **9** in 50 mM Bis–Tris at pH 7.1. During titrations the dilution does not exceed 10%, and all the fluorescence emissions spectra were corrected for dilution. Compound **9** stock solutions were prepared fresh prior to each titration. The dissociation constants for the binding of compound **9** to yeast Magmas was determined by fitting the fluorometric titrations data to Eq. 1, where F_0, F_{SMMI} and $F_{SMMI\infty}$ are the intrinsic fluorescence of free Magmas, compound **9** bound Magmas and Magmas at saturating SMMI 9 concentration, respectively, [*SMMI*] is the total ligand concentration, K_d is the dissociation constant of Magmas–SSMI complex.

$$F_{SMMI} = \left(\frac{F_{FLB\infty}[SMMI]}{K_d + [SMMI]}\right) + F_0 \quad (1)$$

Structural modeling was performed using ICM-Molsoft LLC software. The binding mode for compound **9** was predicted by systematic docking calculations with the ICM software accounting for both ligand and protein flexibility.[12] Docking of compound **9** to individual Tim14 and Tim16 monomers the Tim14–Tim16 heterodimer was modeled using data from PDB entry 2GUZ.[5a]

Reduced Magmas function caused by siRNA knockdown or by mutations in Magmas causes growth inhibition and cell cycle arrest. To assay whether the compounds were active we measured their ability to inhibit yeast proliferation. Yeast is a good organism to test SMMI activity because Magmas is fully functional in *TIM16* null yeast and because the target region is identical across all eukaryotic species.

The concentration dependent effects of the compounds on yeast proliferation are shown in Table 1 (for detail, please see Supplementary data) Compound **5** was inactive at all concentrations while all the other compounds completely inhibited yeast proliferation at 100 μM. At 10 μM, **6** was partially inhibitory and **9** fully inhibited growth. The lead compound **9**, was further tested to determine the lower range of activity (Fig. 1). Compound **9** at 3 μM had a proliferation profile similar to that observed without inhibitor. In contrast, significant and reproducible inhibition was observed at 4 μM, and resulted a lengthening of the time to half maximal growth by 1.8 times.

To genetically demonstrate that effects of **9** were mediated through Magmas, yeast strains containing several different Magmas mutations expressed on a plasmid were screened for altered compound **9** concentration dependent growth. All of these stains express similar levels of Magmas protein, which is approximately four-fold higher than the haploid control (wt genomic) (Short and Jubinsky, unpublished data). Comparing the dose response of wt genomic (*TIM16*) to wt plasmid (human Magmas) showed that

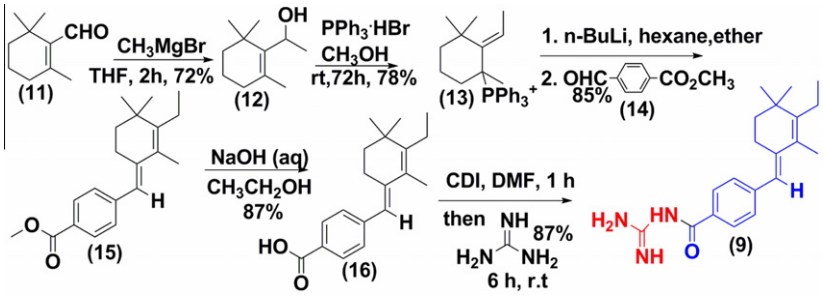

Scheme 2. Synthesis of compound **9**. Compound **9** was synthesized from acid 16.

over-expression of Magmas reduces sensitivity of yeast to SMMI **9** (Supplementary Fig. 1). Yeast strains containing Magmas N84T proliferate identically to wt plasmid without SMMI present, but had an increased resistance to compound **9**. In contrast, yeast strains containing the Magmas A104S mutation are more sensitive to the effects of SMMI **9**.

We have also cultured cell lines with **9** and observed that the morphological and biochemical features were similar to those in cells with siRNA-mediated reduced Magmas expression, providing additional evidence of target specificity (Roy and Jubinsky, unpublished data).

To test whether SMMI directly binds to Magmas compound **9**, the SMMI with the highest biological activity in vivo, was used in a fluorometric titration of Magmas (Fig. 2). The intrinsic fluorescence properties of Magmas with 1 tryptophan and 5 tyrosine residues, upon excitation at 295 nm showed emission maximum centered at 365 nm and a shoulder at ~315 nm, consistent with the fluorescence emission maxima for tryptophan (typically at 340 nm) and tyrosine (typically at 310 nm), respectively. This significant red-shift (15 and 5 nm for tryptophan and tyrosine fluorescence, respectively) suggests solvent exposed Trp and Tyr residues in Magmas.

The fluorometric titration of Magmas with compound **9** showed linear decrease in both tryptophan and tyrosine intrinsic fluorescence intensity with a single isosbestic point at ~420 nm, consistent with a single step binding process of SMMI to yeast Magmas. The ~4-fold quenching of the tryptophan and tyrosine intrinsic fluorescence at saturating SMMI concentration suggest polarity (hydrophobic) changes in the environment of Trp and Tyr upon SMMI **9** binding to Magmas.[11] A dissociation constant (K_d) of 33.5 ± 3.5 μM was determined for the binding of compound **9** to yeast magmas by fitting the titration data to Eq. 1 (Fig. 3, insert). The dissociation constant obtained from the binding of compound **9** to murine Magmas was similar (36 μM).

Molecular modeling of SMMI docking to Tim14 and Tim16 monomers and the Tim14-Tim16 heterodimer showed that the lowest energy binding resulted with the Tim14-Tim16 complex.[14] Lowest energy binding was found with the Tim14–Tlim16 complex. Compound **9** was predicted to bind at the dimer interface establishing multiple hydrophobic contacts with both Tim14 (L100, K111, L114, Q115, and T120) and Tim16 (F95) residues (Fig. 3) and hydrogen bonding Tim14 (E121 and K168).

Table 1
Inhibition of yeast proliferation by five different synthesized compounds

Compound	1 mM	100 μM	10 μM	1 μM
5	–	–	–	–
4	i	+	–	–
6	+	+	±	–
8	i	+	–	–
9	+	+	+	–

(+) Complete inhibition (no proliferation).
(–) No inhibition (normal proliferation).
(±) Partial inhibition.
(i) Compound insoluble.

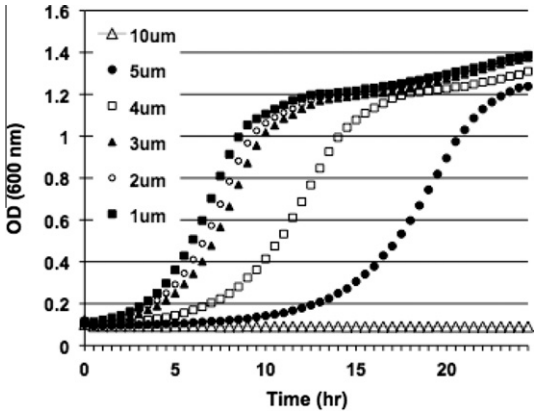

Figure 1. Dose response of compound **9** on yeast proliferation. Yeast cells were cultured in the indicated concentration of SMMI **9** and the optical density was measured.

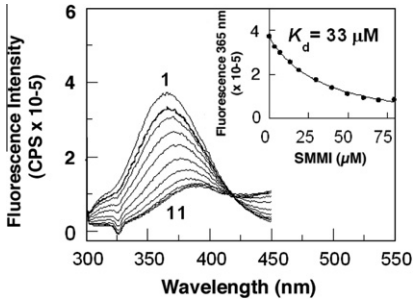

Figure 2. Compound **9** binding to Magmas. Fluorescence emission spectra (λ_x = 295 nm) of yeast Magmas during the fluorometric titration of SMMI in a concentration range between 0 (curve 1) and 79.36 μM (curve 11). Inset, fluorescence emission intensity values at 365 as a function of SMMI 9. The curve is a fit of the data to Eq. 1. Fluorescence emission spectra were recorded at protein concentration of ~3 μM in Bis–Tris (50 mM, pH 7.1, 25 °C).

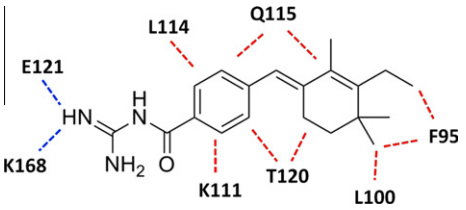

Figure 3. 2-Dimentional-interaction diagram of predicted binding contacts between compound and the Tim14–Tim16 heterodimer. (hydrophobic contact: red; hydrogen bond: blue). Compound **9** establishes multiple hydrophobic contacts with Tim16 (F95) and Tim14 (L100, K111, L114, Q115, and T120). L100 is located at the Tim14 N-terminal arm. The guanidinium moiety forms hydrogen bonds with E121 and K168. Residue numbers are those used in PDB entry 2GUZ.[5a]

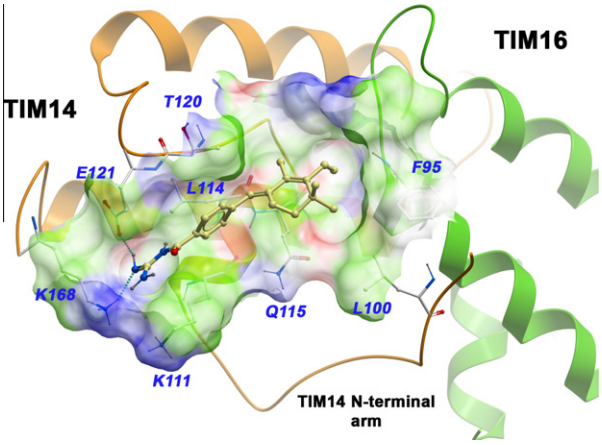

Figure 4. Model of SMMI 9 binding in the Tim14–Tim16 interface pocket. The predicted Tim14–Tim16 binding pocket surface is color coded according to protein binding properties (white: neutral surface; green: hydrophobic surface; red: hydrogen bonding acceptor potential; blue: hydrogen bond donor potential; brown; SMMI **9**).

Steric and physicochemical complementarity between compound **9** and the Tim14–Tim16 heterodimer interface was observed in the model (Fig. 4). Because the hydrophobic substituted cyclohexyl appears to interact with residues (F95 and L100) that stabilize the heterodimer through multiple van der Walls interactions, it is predicted that compound **9** binding results in complex dissociation. In addition, compound **9** likely interferes with the N-terminal arm of Tim14 that interacts with Tim16 helix III, known to be necessary for complex formation and function.[5a]

The binding mode prediction supports the importance of a hydrophilic guanidinium moiety to correctly align the small molecule at the dimer interface, along with hydrophobic groups at the opposite end of the molecule to induce an alternative conformation for the N-terminal arm of Tim14. Confirmation of this model by NMR, Magmas mutagenesis and crystal structures are planned.

Several SMMIs that are biologically active in yeast were synthesized. Over-expression of Magmas and the isolation of Magmas mutants with both increased and decreased sensitivity to **9** showed that Magmas is a target in vivo, while the fluorometric titration experiments demonstrated a direct physical interaction. We also showed that compound **9** is predicted to functionally interact with Magmas using computational modeling. SMMIs should prove useful for studying mitochondrial function and may have clinical relevance for a variety of human diseases. The effects of SMMI on CNS malignancies are under evaluation, as are efforts to develop agents that can monitor Magmas function in vivo.

Acknowledgements

This study was supported by the James B. Ax Family Foundation. We thank E. Richard Stanley and Donna Alex for their continued encouragement and Ruben Abagyan and Macro Neves for their assistance with the modeling of SMMI and Magmas.

Supplementary data

Supplementary data associated with this article can be found, in the online version, at doi:10.1016/j.bmcl.2011.03.050.

References and notes

1. Jubinsky, P. T.; Messer, A.; Bender, J.; Morris, R. E.; Ciraolo, G. M.; Witte, D. P.; Hawley, R. G.; Short, M. K. *Exp. Hematol.* **2001**, *29*, 1392.
2. Jubinsky, P. T.; Short, M. K.; Mutema, G.; Witte, D. P. *J. Histochem. Cytochem.* **2003**, *51*, 585.
3. Peng, J.; Huang, C. H.; Short, M. K.; Jubinsky, P. T. *In Silico Biol.* **2005**, *5*, 251.
4. (a) Li, Y.; Dudek, J.; Guiard, B.; Pfanner, N.; Rehling, P.; Voos, W. *J. Biol. Chem.* **2004**, *279*, 38047; (b) D'Silva, P. R.; Schilke, B.; Walter, W.; Craig, E. A. *Proc. Natl. Acad. Sci. U.S.A.* **2005**, *102*, 12419; (c) Frazier, A. E.; Dudek, J.; Guiard, B.; Voos, W.; Li, Y.; Lind, M.; Meisinger, C.; Geissler, A.; Sickmann, A.; Meyer, H. E.; Bilanchone, V.; Cumsky, M. G.; Truscott, K. N.; Pfanner, N.; Rehling, P. *Nat. Struct. Mol. Biol.* **2004**, *11*, 226.
5. (a) Mokranjac, D.; Bourenkov, G.; Hell, K.; Neupert, W.; Groll, M. *EMBO J.* **2006**, *25*, 4675; (b) Kozany, C.; Mokranjac, D.; Sichting, M.; Neupert, W.; Hell, K. *Nat. Struct. Mol. Biol.* **2004**, *11*, 234.
6. Jubinsky, P. T.; Short, M. K.; Mutema, G.; Morris, R. E.; Ciraolo, G. M.; Li, M. *J. Mol. Histol.* **2005**, *36*, 69.
7. (a) van de Vijver, M. J.; He, Y. D.; Van't Veer, L. J.; Dai, H.; Hart, A. A.; Voskuil, D. W.; Schreiber, G. J.; Peterse, J. L.; Roberts, C.; Marton, M. J.; Parrish, M.; Atsma, D.; Witteveen, A.; Glas, A.; Delahaye, L.; van der Velde, T.; Bartelink, H.; Rodenhuis, S.; Rutgers, E. T.; Friend, S. H.; Bernards, R. N. *Engl. J. Med.* **2002**, *347*, 1999; (b) Desmedt, C.; Piette, F.; Loi, S.; Wang, Y.; Lallemand, F.; Haibe-Kains, B.; Viale, G.; Delorenzi, M.; Zhang, Y.; d'Assignies, M. S.; Bergh, J.; Lidereau, R.; Ellis, P.; Harris, A. L.; Klijn, J. G.; Foekens, J. A.; Cardoso, F.; Piccart, M. J.; Buyse, M.; Sotiriou, C. *Clin. Cancer Res.* **2007**, *13*, 3207; (c) Tagliati, F.; Gentilin, E.; Buratto, M.; Mole, D.; degli Uberti, E. C.; Zatelli, M. C. *Endocrinology* **2010**, *151*, 4635.
8. (a) Sinha, D.; Joshi, N.; Chittoor, B.; Samji, P.; D'Silva, P. *Human Mol. Genet.* **2010**, *19*, 1248; (b) Elsner, S.; Simian, D.; Iosefson, O.; Marom, M.; Azem, A. *Int. J. Mol. Sci.* **2009**, *10*, 2041.
9. (a) Shridhar, D. R.; Reddy Sastry, C. V.; Bansal, O. P.; Pulla Rao, P. P. *Synthesis* **1981**, *19*, 2; (b) Liu, F.; Evans, T.; Das, B. C. *Tetrahedron Lett.* **2008**, *49*, 1578.
10. *Detail experimental procedures for compound* (**9**): The syntheis of acid **16** involves the reaction with methyl magnesium bromide with β-cyclocitral in THF to give the alcohol as a yellow oil.[13] The alcohol gave satisfactory spectral data and was directly converted to the triphenyl phosphine salt by treatment with triphenylphosphine hydrobromide in methanol. Recrystalization of the salt from methanol/ether (1:6) gave a yellow crystalline solid.[14] Formation of the Witting reagent from the salt in ether was accomplished with *n*-butyllithium in hexane at room temperature (dark-red color). The Witting reagent was treated with methyl 4-formybenoate in ether at −78 °C for 10–15 min and then stirred at room temperature under a nitrogen atmosphere for 30 h. The crude ester was purified by flash column chromatography (hexane/ethyl acetate: 98:2) to give a brown oil in 85% yield.[15] The ester was saponified to generate a white solid which was filtered, washed with water, and dried. The product was recrystallized from hot ethanol and washed with dry hexane to give acid as white crystals (87%) yield. The structure was confirmed by ^{1}H, ^{13}C NMR and NOE experiment, HMBC, and HRMS. A mixture of acid **16** (300 mg;1.05 mmol) in dry DMF (4 mL) and CDI (171 mg;1.05 mmol) was stirred at room temperature under nitrogen atmosphere for 1 h. Guanidine base was prepared by consecutive additive of sodium-*tert*-butoxide (201.8 mg, 2.1 mmol) and guanidine hydrochloride (200 mg, 2.1 mmol) to a dry mixture of dimethylformamide/dioxane (1:1, 8 mL) under nitrogen, this mixture was heated to 50–55 °C for 20 min, and then the NaCl was filtered. The solution of CDI and acid was added to the guanidine base solution. The mixture was stirred at room temperature for 6 h. The progress of the reaction was monitored by TLC. After the reaction was completed the mixture was evaporated and the DMF was removed under vaccum. The residue suspended in cold water (8 mL). The crystaline solid was filtered, washed with water, and dried, then purified by fractional crystalization from methanol to give a white solid 340 mg (87%). Mp: 165–167 °C. ^{1}H NMR (300 MHz, acetone-d_6): 7.90–7.82(d, J = 8.0 Hz, 2H), 7.40 (d, J = 8 Hz, 2H), 6.47(s, 1H);2.55 (m, 2H), 2.19 (q, 3H), 1.86 (s, 3H);1.44 (m, 2H), 1.05 (s, 6H) and 1.03 (t, J = 8 Hz, 3H) ^{13}C NMR $CDCl_3$: 177.2;163.8, 147.6, 141.5, 140.9, 137.2, 129.06, 128.7, 127.5, 121.6, 39.1, 35.9, 28.6, 27.5, 24.4, 22.9, 14.9 and 14.6 ESI-MS: Calcd for $C_{20}H_{27}N_3O$ ($[M+H]^+$) 326.2227; found: 326.2223.
11. Boeke, J. D.; Trueheart, J.; Natsoulis, G.; Fink, G. R. *Methods Enzymol.* **1987**, *154*, 164.
12. Totrov, M.; Abagyan, R. *Proteins* **1997**, Suppl 1, 215.
13. Fernandez-Mateos, A.; Mateos Buron, L.; Martin de la Nava, E. M.; Rubio Gonzalez, R. *J. Org. Chem.* **2003**, *68*, 3585.
14. Rosenberger, M.; Neukom, C. *J. Org. Chem.* **1982**, *47*, 1782.
15. Waugh, K. M.; Berlin, K. D.; Ford, W. T.; Holt, E. M.; Carrol, J. P.; Schomber, P. R.; Thompson, M. D.; Schiff, L. J. *J. Med. Chem.* **1985**, *28*, 116.